
DEEP LEARNING IN A BILATERAL BRAIN WITH HEMISPHERIC SPECIALIZATION

✉ **Chandramouli Rajagopalan**
 Cerenaut
 Melbourne, Australia
 chanduiyer.raja@gmail.com

✉ **David Rawlinson**
 Cerenaut
 Melbourne, Australia
 dave@cerenaut.ai

✉ **Elkhonon Goldberg**
 Luria Neuroscience Institute
 & NYU Grossman School of Medicine
 New York City, USA
 eg@elkhonongoldberg.com

✉ **Gideon Kowadlo**
 Cerenaut
 Melbourne, Australia
 gideon@cerenaut.ai

ABSTRACT

The brains of all bilaterally symmetric animals on Earth are divided into left and right hemispheres. The anatomy and functionality of the hemispheres have a large degree of overlap, but there are asymmetries and they specialise to possess different attributes. Other authors have used computational models to mimic hemispheric asymmetries with a focus on reproducing human data on semantic and visual processing tasks. We took a different approach and aimed to understand how dual hemispheres in a bilateral architecture interact to perform well in a given task. We propose a bilateral artificial neural network that imitates lateralisation observed in nature: that the left hemisphere specialises in specificity and the right in generality. We used different training objectives to achieve the desired specialisation and tested it on an image classification task with two different CNN backbones – ResNet and VGG. Our analysis found that the hemispheres represent complementary features that are exploited by a network head which implements a type of weighted attention. The bilateral architecture outperformed a range of baselines of similar representational capacity that don't exploit differential specialisation, with the exception of a conventional ensemble of unilateral networks trained on a dual training objective for specifics and generalities. The results demonstrate the efficacy of bilateralism, contribute to the discussion of bilateralism in biological brains and the principle may serve as an inductive bias for new AI systems.

Keywords Bilateral · Hemispheric specialisation · Hemispheric asymmetry · Brain-inspired architecture · Cognitive architectures · Deep learning · Computational cognitive neuroscience · Inductive bias

1 Introduction

Left and right hemispheres are a remarkably conserved feature of brains across species, suggesting their importance for intelligence. The anatomy and functionality of the hemispheres have a large degree of overlap, but they are asymmetric and specialise to possess different attributes. For example, the left hemisphere is specialised for specific (fine) classes and familiarity/routine whereas the right hemisphere is specialised for more general (coarse) classes and novelty [4, 5].

Researchers have studied the bilateral brain with computational models that mimic anatomical and functional asymmetries. The models are typically subjected to standard tasks and compared to human behavioural data. The various studies provide evidence that asymmetric functional and anatomical differences can give rise to observed lateralisation of activity (i.e. specialisation) for specific tasks e.g. [1, 18, 13, 8, 11].

The central question of existing models is to understand the cause of the observed specialisation. The aim of this project is to investigate a different question – what is the benefit of specialised hemispheres and how do they complement each other for a given task? Our approach is to induce specialisation directly, rather than test if it emerges as a result of architectural asymmetry. Our objective is to develop a theory of operation and to understand how bilateral principles could be exploited for AI/ML.

1.1 Our approach

We focused on the left hemisphere’s specialisation on specifics, and the right’s specialisation on generalities [4, 5]. We hypothesised that an ANN with differentially specialised sub-networks would outperform a single comparable network in a classification task featuring both fine and coarse class labels. We predicted that with specialisation, the hemispheres would extract distinct but overlapping features, despite identical observations. In addition, we expected that a bilateral architecture would be able to combine these features to improve overall accuracy.

We chose a hierarchical image classification task where each sample belongs to both a fine and a coarse class e.g. **coarse**: sea creature, **fine**: penguin, seal, shark. We modelled the hemispheres with left and right CNNs and induced specialisation using supervised training with different objectives, using either coarse or fine labels. The bilateral network was compared to several comparative baselines that do not have specialisation but do have the same number of learnable parameters. The differences were analysed to explore the effects of bilateral specialisation. Experiments were repeated with two types of CNN hemispheres, VGG and ResNet variants, to test generalisation over different backbones.

The source code is available at [7].

2 Related work

Biologically inspired multi-network architectures [20] created a dual-stream architecture called Neuromodulator Meta-learner, where one network learns to modulate the other, to enhance continual learning. [21] created a network with parallel pathways to reproduce the functionality of dorsal (‘where’) and ventral (‘what’) pathways in an ANN trained with a single loss function. [22] discussed specialisation of a branched neural network.

In the most related study, [19] tackled the same image classification task with fine and coarse (hierarchical) classes. The authors created a single network with two hemispheres, and trained it with supervised learning and a single loss function. They used hyperparameters with analogies to biological parameters in each hemisphere to encourage specialisation. Specialisation was achieved in each side but the bilateral network did not have an advantage over baselines.

Ensemble models Our bilateral approach can be viewed as a type of ensemble, which is a popular approach in ML [23]. Typically, the outputs of multiple models, trained on different seeds, are combined; and the models are of the same type. Other techniques encourage diversity within the ensemble using different training objectives, sampling, architecture, or losses [24, 25, 26]. Our work can be viewed as a special case of a diversified ensemble, where the ensemble architecture exploits hierarchical data labels to achieve diversification.

Multi-domain learning In multi-domain learning (MDL), multiple models are trained to specialise in a particular domain [27]. Two of the main approaches include a) modelling domain-specific and domain-general features [28] and b) explicitly modelling the relationship between domains. MDL is focused on classes from domains with different distributions. The domain is sometimes explicit and other times it is determined by the model [29]. In contrast, this project is focused on explicit hierarchical labels from the same distribution. The objective being to mimic learning different aspects of a single task with left and right hemispheres (2 separate models).

3 Models

We compared a bilateral model to several baselines. Each model consisted of one or more feature extractor, representing hemispheres, as well as one or two classifier heads, one for each label type (fine or coarse). The hemispheres were implemented with two different CNN architectures to test if the effects generalise across architectures: ResNet [35] and VGG [36]. We chose VGG and ResNet because they are common, well understood and amongst the best performing on many vision tasks.

In the case of ResNet-based models, we empirically optimised the number of layers on the dataset, resulting in a 9-layer network, hereafter referred to as ResNet-9. In shorthand, the full architecture is: **conv64-conv128-pool-res128,128-pool-conv256-conv512-pool-res512,512-av_pool**. ConvX = convolutional with X filters, res = residual block with two

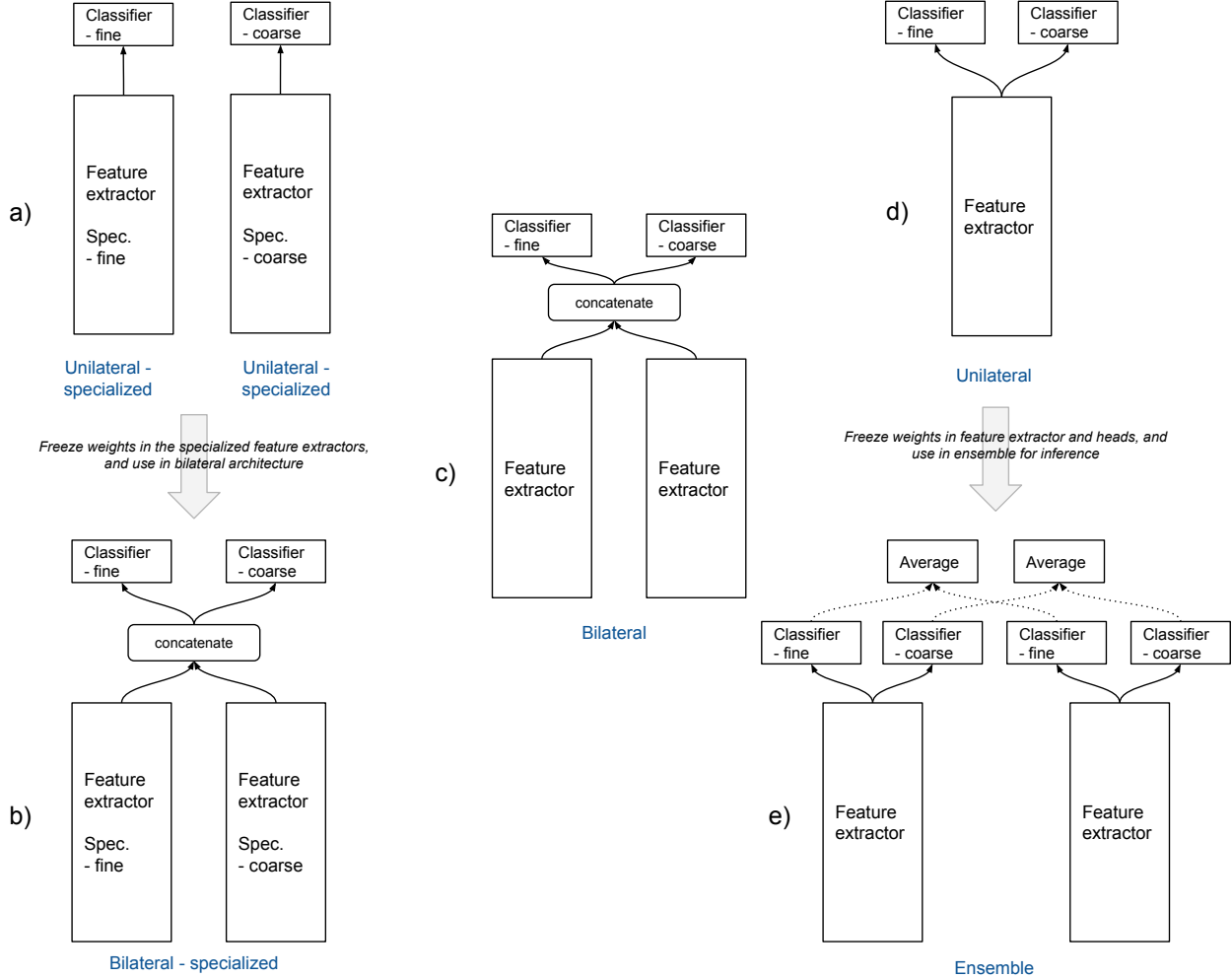


Figure 1: **The range of models.** Feature extractors are either ResNet-9 or VGG-11. The classifier heads are single layer fully connected networks, with output dimensions the same size as the number of classes. For brevity, if not specified, the network is unspecialised.

convolutional blocks of X,Y filters, pool = max pool, av_pool = average pool. All filters are 3x3 and we used ReLU activation function.

For the VGG model, we chose the VGG-11A variant [36], hereafter referred to as VGG-11, as it is closest in depth to ResNet-9 and works well for CIFAR-100 [37]. We used the PyTorch implementation, but removed the final fully-connected layer as we added our own classifier (explained below). In shorthand, the full architecture is: **conv64-pool-conv128-pool-conv256-conv256-pool-conv512-conv512-pool-conv512-conv512-pool-fc4096-fc4096**. Definitions as above, and fcX = fully connected with X units. All filters are 3x3. Although VGG-11 and ResNet-9 are both convolutional networks with a similar depth, there are substantial architectural differences. VGG does not have skip connections, and there are a lot more parameters due to the fully-connected layers.

The heads consist of a single fully-connected layer, without bias or non-linearity and with output dimensions the same size as the number of classes (10 for coarse and 100 for fine).

The models are depicted in Figure 1 and described below. Details on training and evaluation in Section 4.1.2.

3.1 Bilateral network - specialised

Assembling and training the network consisted of two phases. In Phase 1, individual hemispheres were trained to be specialised feature extractors using supervised learning with a single classifier head, resulting in ‘Unilateral -

specialised’, Figure 1a. The left was specialised for specific classes using fine labels, and the right for general classes with coarse labels. In Phase 2, the hemispheres (serving as feature extractors) were brought together into a broader architecture, with two initialised classifier heads, one for fine and coarse labels, resulting in ‘Bilateral - specialised’, Figure 1b, . The weights of the individual hemispheres were frozen and the heads were trained to use the features for classifying fine and coarse labels. A single loss was calculated by adding the loss from each head.

3.2 Baseline models

Unilateral networks with specialisation We compared the bilateral network to the individual specialised hemispheres alone, on the tasks for which they were specialised, referred to as Unilateral-specialised, Figure 1a. Specialisation was achieved using supervised training with selective labels as described in Section 3.1.

Unilateral network without specialisation To investigate specialisation, we compared Unilateral-specialised to a single hemisphere *without* specialisation, referred to as Unilateral-unspecialised, Figure 1d. The single hemisphere was trained on both types of labels simultaneously, by using two classifier heads and adding the loss. This baseline also helps to understand the effect of complementary loss functions; on a single hemisphere compared to the bilateral network.

Bilateral network without specialisation To better understand the role of specialisation in the bilateral network, we compared Bilateral-specialised to an equivalent network, with the same number of trainable parameters, but without specialisation, referred to as Bilateral-unspecialised, Figure 1c. It can be viewed as a type of ensemble, where the models are combined in the same way as the specialised bilateral network.

We trained the entire network (two hemispheres and two heads) without first explicitly inducing specialisation in the individual hemispheres. Like for the unilateral network and bilateral network with specialisation, the loss from each head are added together to create a single loss.

Ensembles To understand the differences between differential specialisation and conventional ensembling, we compared to a 2-model ensemble, Figure 1e. We chose 2 models, so that the ensemble has approximately the same number of trainable parameters as the bilateral network. We used two unilateral models without specialisation, trained from different seeds. The output of the ensemble was the average from the heads: for fine classification, the average of the fine heads, and for coarse, the average of the coarse heads. We trained five models with different seeds, and then constructed five 2-model ensembles, each with a unique pair of models selected from the pool of five.

4 Experiments

4.1 Experimental setup

4.1.1 Dataset

We used the CIFAR-100 dataset [30], as it includes hierarchical labels that denote fine (specific) and coarse (general) classes. The dataset is split into 50,000 training and 10,000 test samples. Images were resized to 32x32 and we used two widely adopted data augmentation techniques, a random crop and a random horizontal flip (using the inbuilt PyTorch functions) to increase the diversity of the training set.

4.1.2 Training and evaluation

The models were trained with supervised learning using a cross-entropy loss function. In the case of dual heads (one with each label type, see Section 3), the loss from each head was added to create a single loss value. Weights were initialised with PyTorch defaults, from a random uniform distribution $U(-\sqrt{k}, \sqrt{k})$: for linear layers $k = 1/in_features$, and for the convolutional layers $k = \frac{1}{C_{in} * \prod_{i=0}^1 kernel_size[i]}$. We used weight decay of 1.0e-5, dropout of 0.6 on the classifier heads to regularise the models, Adam [39] for optimisation, with a learning rate of 1.0e-4 and a mini-batch size of 256.

Each network was trained for 180 epochs from 5 random seeds. At the end of each epoch, the models were validated on the test split. The number of epochs was sufficient to ensure that the validation accuracy had plateaued, and the final model was the one with the highest validation accuracy across epochs.

4.1.3 Framework and computational resources

Experiments were conducted with the PyTorch-Lightning [40] research framework, a wrapper around the PyTorch library [41]. All models were trained and evaluated with a virtual machine with a single NVIDIA A10 GPU, 24GB RAM (through Lambda Labs <https://lambdalabs.com/>).

4.2 Visualising network operation

We focused on one backbone, ResNet-9, and used two types of visualisations to better understand the operation of the bilateral network. To be informative, we selected key scenarios that are distinct from each other and highlight the contribution of different parts of the network, described below. The definition of ‘correct’ for the bilateral-specialised network, is that it was successful for both fine and coarse class labels.

- Scenario 1: Bilateral-specialised network is correct, left and right hemispheres are incorrect
- Scenario 2: Bilateral-specialised network and right hemisphere are correct, left hemisphere is incorrect
- Scenario 3: Bilateral-specialised network and left hemisphere are correct, right hemisphere is incorrect
- Scenario 4: Bilateral-specialised network is incorrect, left and right hemispheres are correct

Gradient camera (Grad-Cam) visualisation To understand how the specialised bilateral network exploits features from both hemispheres, we visualised gradient flow with respect to target convolutional layers [43, 42] using the Grad-Cam library [44]. The gradients reveal which areas of the image contribute most to the prediction; the gradient heatmap highlights the region of focus. We applied the visualisation to each of the specialised hemispheres individually, and compared it to the bilateral network.

For a single hemisphere, the gradients were averaged over the 2nd convolutional layer of each residual block (2 convolutional layers with skip connections) during prediction. In the case of the bilateral network, the gradients were averaged over both hemispheres during simultaneous prediction of both coarse and fine labels (the network had two heads).

Feature analysis using cosine similarity We investigated how left and right features are exploited by the bilateral network by analysing the relationship between representations in different parts of the network, with a focus on how the representations are transformed by the network heads. We did this by measuring the similarity of features for images of the same label. They are expected to have similar features, so measuring the feature similarity at different parts of the network should be revealing.

We first grouped the image samples into random pairs with the same class label. We then plotted a bivariate distribution of cosine similarity between the pairs, one for the input to the heads, denoted ‘concatenated’ and the other for the average of the network head outputs, denoted ‘bilateral’. Similarity is plotted along the following dimensions: left hemisphere, right hemisphere and a third dimension, either concatenated or bilateral. Additionally, univariate marginal distributions were plotted for each hemisphere.

5 Results

5.1 Accuracy

The relative performance of models was very consistent between ResNet and VGG backbones, Tables 1 and 2 and Figures 2 and 3. Accuracy given as mean \pm 1 standard deviation (shown as error bars in the plots) of 5 seeds. In summary, Bilateral-specialised outperformed all the baselines, except for the 2-model ensemble. The 2-model ensemble consists of unilateral models, which were more effective than specialised unilateral models in most cases. The exception was the VGG backbone with coarse labels, where the unspecialised unilateral model was not better than the specialised version, and the resulting 2-model ensemble did not outperform Bilateral-specialised.

5.2 Visualising network operation

The Grad-Cam visualisations are shown in Figures 4 to 7 for the scenarios described in Section 4.2. In general, the features appear to be more local in the left hemisphere and more global in the right. The heads blend different aspects of features from the left and right, for the task. The effect is that in many cases, **features trained for fine classes are helpful for coarse classes and vice versa, and a correct classification can be achieved even if both hemispheres are individually incorrect**.

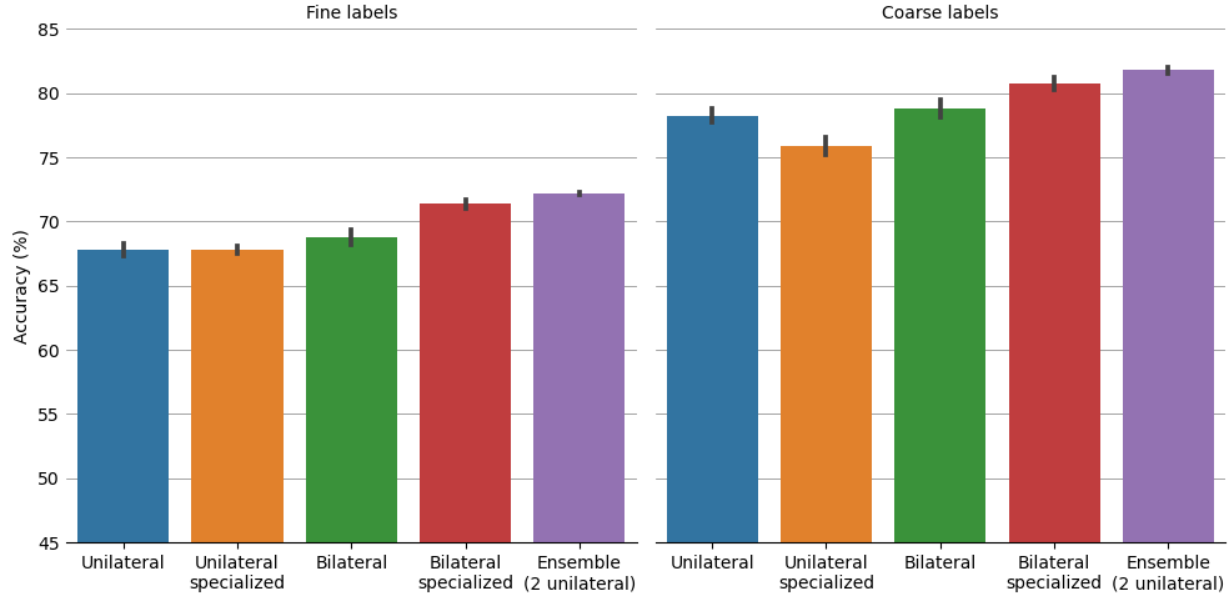


Figure 2: Accuracy of ResNet-based models. For brevity, if not specified, the network is unspecialised.

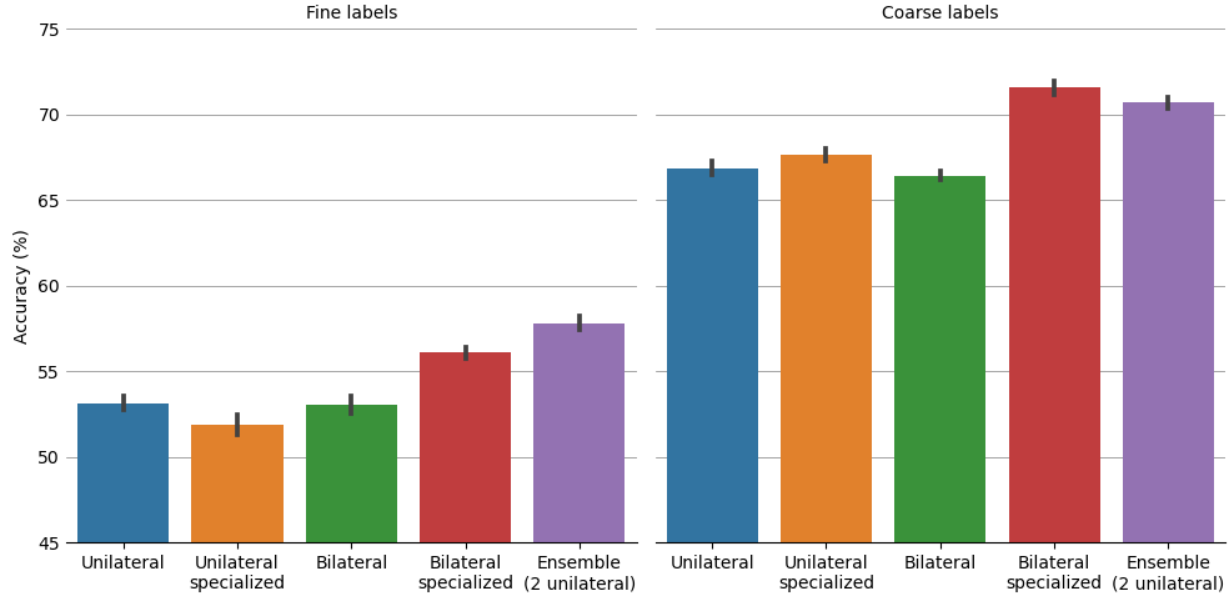


Figure 3: Accuracy of VGG-11-based models. For brevity, if not specified, the network is unspecialised.

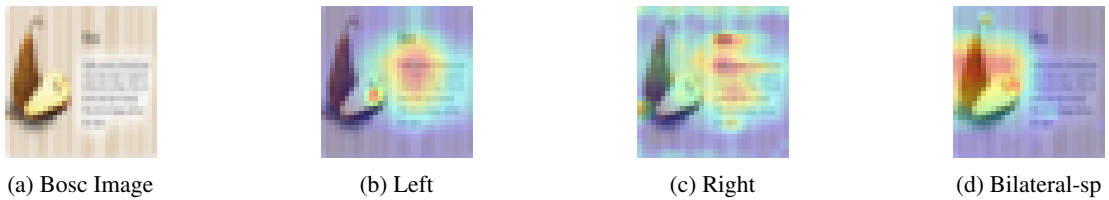


Figure 4: **Grad-Cam for Scenario 1: The bilateral-specialised (abbreviated to bilateral-sp in the figure) network is correct, left and right are incorrect.** The bilateral network appears to adjust the area of focus even when both the hemispheres' features are situated external to the bosc.

Model	# Params (M)	Accuracy (%) - fine labels	Accuracy (%) - coarse labels
Unilateral	6.63	67.81 ± 0.46	78.25 ± 0.51
Unilateral-specialised	6.58	67.81 ± 0.31	—
Unilateral-specialised	6.62	—	75.87 ± 0.70
Bilateral	13.26	68.80 ± 0.59	78.82 ± 0.65
Bilateral-specialised	13.26	71.35 ± 0.36	80.71 ± 0.48
Ensemble (2 unilateral models)	13.26	72.15 ± 0.11	81.80 ± 0.24

Table 1: Accuracy of ResNet-based models.

Model	# Params (M)	Accuracy (%) - fine labels	Accuracy (%) - coarse labels
Unilateral	129.26	53.13 ± 0.41	66.86 ± 0.41
Unilateral-specialised	129.18	51.87 ± 0.58	—
Unilateral-specialised	128.85	—	66.86 ± 0.41
Bilateral	258.52	53.05 ± 0.49	66.42 ± 0.27
Bilateral-specialised	258.52	56.09 ± 0.33	71.57 ± 0.42
Ensemble (2 unilateral models)	258.52	57.81 ± 0.38	70.68 ± 0.30

Table 2: Accuracy of VGG-based models

The cosine similarity results are shown in Figure 8 and Figure 9. In the concatenated distribution, there is a strong correlation between similarity in left and concatenated, and right and concatenated. In contrast, there is no obvious correlation in the bilateral distribution. The network heads appear to have learned a non-linear transformation of the feature space.

6 Discussion

We found that there is an advantage of two hemispheres over one, demonstrated by the fact that the specialised bilateral architecture (Bilateral-specialised) outperformed individual hemispheres (Unilateral-specialised and Unilateral). Furthermore, we found that it is not due to the greater number of learnable parameters, and having two hemispheres is not sufficient, but that specialisation is important, shown by the benefit of Bilateral-specialised over Bilateral.

Surprisingly, unspecialised hemispheres (Unilateral) performed as well or better than specialised hemispheres (Unilateral-specialised) in most cases. Training with two objective functions (fine and coarse) led to better performance on both labels – whether that is in a bilateral or unilateral architecture.

Ultimately, two hemispheres arranged into a conventional ensemble achieved the best results. A key difference with Bilateral-specialised, is that the component models were more effective to begin with. Another difference is the way in which the model outputs are combined – averaging of the classification vs concatenation of the feature vector. Future work could explore this in more detail.

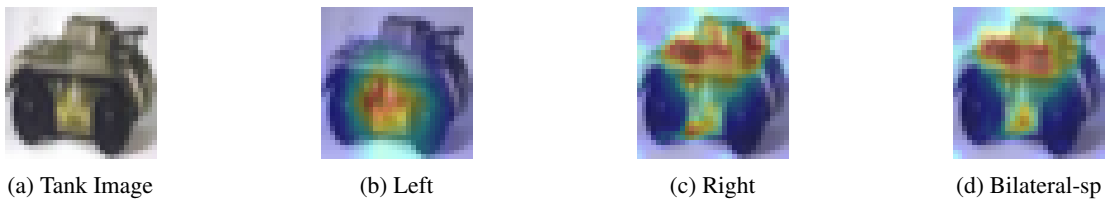


Figure 5: **Grad-Cam for Scenario 2: The bilateral-specialised network and the right are correct, the left is incorrect.** Possibly due to the fact that there are multiple labels with wheels, the left failed to differentiate the tank by its wheels alone, however the bilateral model appears to overcome this, using the right's features.



Figure 6: **Grad-Cam for Scenario 3: The bilateral-specialised network and the left are correct, the right is incorrect.** The left hemisphere identified more local features of the bicycle compared to the right. The network head appear to exploit the left representations to make an accurate prediction.



Figure 7: **Grad-Cam for Scenario 4: The bilateral-specialised network is incorrect, the left and right hemispheres are correct.** Both hemispheres identified local and global features. The network heads appear to over-compensate and focus on the region outside of the sofa, which is ultimately unsuccessful.

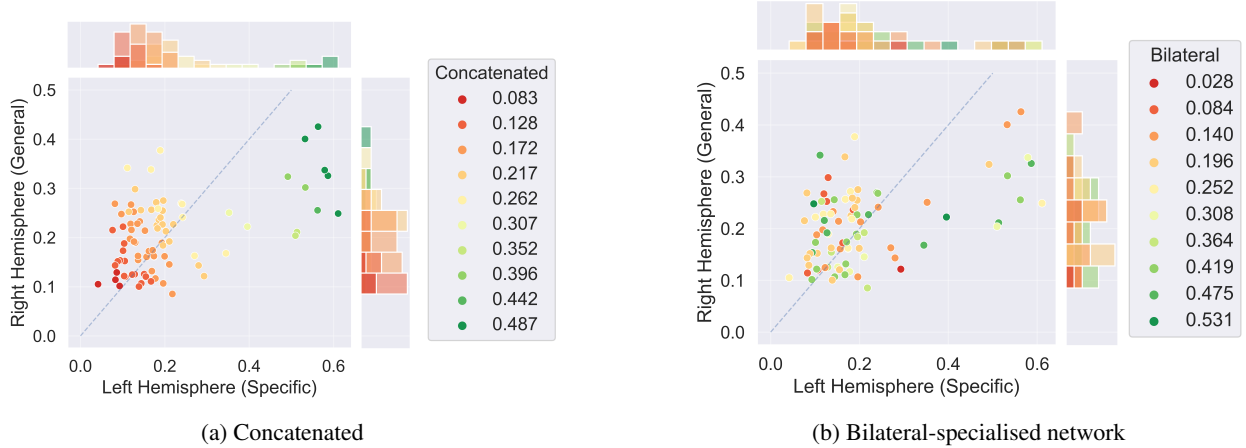


Figure 8: **Cosine similarity distribution for Scenario 1: The bilateral-specialised network is correct, left and right are incorrect.** Many of the pairs (same label) have dissimilar (values closer to 0) features in left and right, seen in the density of points close to the origin. The concatenated features are also dissimilar, but the bilateral network elevates the similarity of many of the points. Each point is a pair of images with the same label. The x-axis is similarity in the left hemisphere, y-axis is similarity in the right hemisphere. The color is similarity in the combined representation. Additionally, the univariate marginal distributions are shown for left and right with histograms above and to the side of the bivariate distribution.

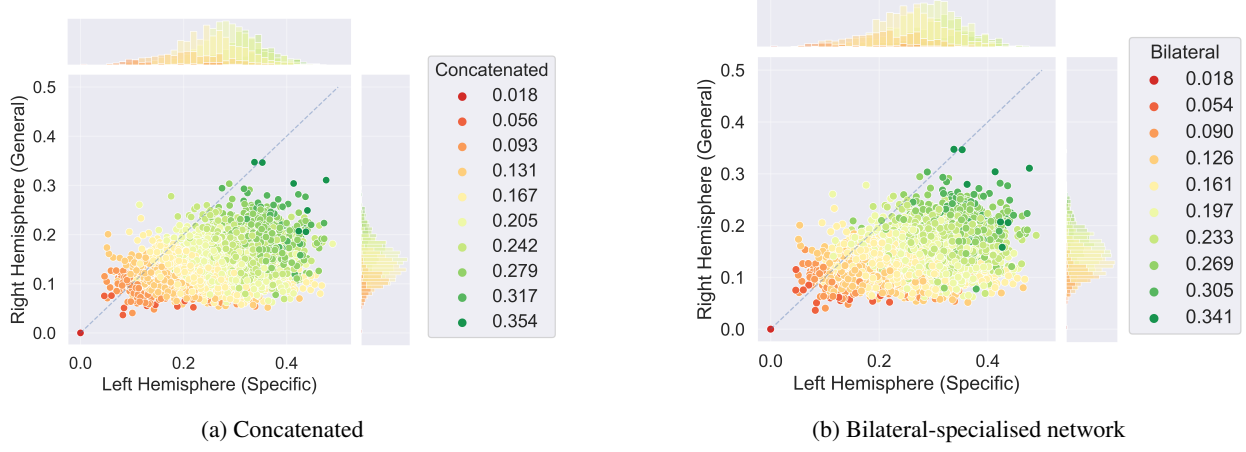


Figure 9: Cosine similarity distribution for Scenario 2: The bilateral-specialised network and the right are correct, the left is incorrect. Some regions with points that have low similarity in the left (at approximately $x, y = 0.2, 0.2$), have elevated similarity in the bilateral output, compared to concatenated. Also, for points with high similarity in the left (approximately 0.35, 0.1), the similarity is lower in the bilateral output. In other words, the bilateral network was able to exploit features in the right hemisphere over the left. Each point is a pair of images with the same label. The x-axis is similarity in the left hemisphere, y-axis is similarity in the right hemisphere. The color is similarity in the combined representation. Additionally, the univariate marginal distributions are shown for left and right with histograms above and to the side of the bivariate distribution.

Both the specialised bilateral network and the ensemble were able to boost performance of individual hemispheres. However, they use different mechanisms.

The novel finding of the paper is that a bilateral architecture can exploit specialised hemispheres, and the remainder of the paper examines this principle.

Computational cost Compared to a conventional single network, the bilateral architecture has approximately double the number of parameters and computational cost. The performance boost between unilateral and specialised bilateral models may appear modest for the additional cost. However, incremental gains are difficult to achieve at high levels of performance, making the 2.5-5% improvement (across fine, coarse and hemisphere architectures) consequential. This is the first study to demonstrate the bilateral principle, and like other new architectures, greater improvements can be expected in the future.

How does the bilateral architecture work? The Grad-Cam images reveal that the left hemisphere extracts more localised features than the right. Different learning objectives enable them to capture different aspects of the environment. Collectively the set of features is greater than one network with one objective. Interestingly, even though the left is explicitly trained on fine labels, the features that it extracts are helpful for coarse classes. The inverse is true of the right.

With reference to the cosine similarity visualisation, before the network heads, the similarity of pairs of images of the same class is correlated with left and right and the similarity is no longer correlated after the network heads; which suggests that the heads implement a non-linear transformation. In many cases, when left or right produce ineffective features, shown by low similarity between embeddings of these images of the same class, the heads are able to produce features that have increased similarity. The network heads learn to combine the features from left and right, to different degrees, to produce better predictions. In some cases, the bilateral network makes a correct classification, even if both hemispheres are individually wrong.

In summary, specialisation creates a higher diversity of features. The network heads implement a type of weighted attention to left and right hemispheres selectively in a task dependent manner, improving overall class prediction.

Relation to biology A limitation of our model, in terms of biological accuracy, was that inter-hemispheric connectivity was achieved at the outputs of the hemispheres. In contrast, biological hemispheres are interconnected throughout their hierarchies [45]. Nevertheless, the heads may serve a similar purpose, albeit in a cruder way. Inter-hemispheric connectivity comprises a complex combination of inhibitory and excitatory projections. The hemisphere that is better able to represent the input is likely to have stronger activation and thus inhibit the other hemisphere [1, 2]. Like the

heads, this too is a type of selectivity. Building a model with interconnected hemispheres throughout the hierarchy is a topic for future research.

The central finding, that left and right hemispheres extracted local and non-local features, to improve performance on a given task, provides one plausible suggestion (and testable hypothesis) for the prevalence of bilateral brains in nature. A possible approach to investigate this idea is with transcranial magnetic stimulation (TMS) to selectively impair one hemisphere at a time on controlled tasks [46].

7 Conclusion

Inspired by our bilateral brains, we built a bilateral architecture with left and right neural networks using two CNN backbones and compared them to baselines that captured distinct characteristics of the proposed bilateral network. We used a classification task with hierarchical classes that captured an observed characteristic of biological hemispheres, that the left is more specialised for fine classes and the right for coarse classes. The hemispheres were trained to specialise on fine and coarse classes accordingly. They extracted specialised features and through a type of ‘weighted attention’ by a simple fully connected layer, outperformed various (but not all) baselines on classification of both fine and coarse classes. The specialised representations had benefits above the explicit objective of their individual hemispheres. The results demonstrate that small procedural changes to training can achieve specialisation, and that specialisation can be complementary and beneficial for certain tasks. The operation of the artificial network provides ideas for the study of neurobiological hemispheric specialisation. Simultaneously, this work shows that neuroscientific principles can provide inductive biases for novel ML architectures. Currently, in the field of AI/ML where scaling of existing architectures is achieving great success, it’s interesting to look at new principles on smaller architecture that could then be scaled.

Acknowledgements

Thanks to Punarjay Chakravarty for helpful discussions.

References

- [1] Natalia Shevtsova and James A. Reggia. A neural network model of lateralization during letter identification. *Journal of Cognitive Neuroscience*, 11:167–181, 1999. ISSN 089892999563300. URL [/record/1999-05033-003](https://doi.org/10.1162/089892999563300).
- [2] Scott A. Weems and James A. Reggia. Hemispheric specialization and independence for word recognition: A comparison of three computational models. *Brain and Language*, 89:554–568, 6 2004. ISSN 0093-934X. doi:[10.1016/J.BANDL.2004.02.001](https://doi.org/10.1016/J.BANDL.2004.02.001).
- [3] Ya Ning Chang and Matthew A. Lambon Ralph. A unified neurocomputational bilateral model of spoken language production in healthy participants and recovery in poststroke aphasia. *Proceedings of the National Academy of Sciences of the United States of America*, 117:32779–32790, 12 2020. ISSN 10916490. doi:[10.1073/PNAS.2010193117/SUPPL_FILE/PNAS.2010193117.SAPP.PDF](https://doi.org/10.1073/PNAS.2010193117/SUPPL_FILE/PNAS.2010193117.SAPP.PDF). URL <https://www.pnas.org/doi/abs/10.1073/pnas.2010193117>.
- [4] Elkhonon Goldberg and Louis D Costa. Hemisphere differences in the acquisition and use of descriptive systems. *Brain and Language*, 14:144–173, 1981. ISSN 0093-934X. doi:[https://doi.org/10.1016/0093-934X\(81\)90072-9](https://doi.org/10.1016/0093-934X(81)90072-9). URL <https://www.sciencedirect.com/science/article/pii/0093934X81900729>.
- [5] E. Goldberg, K. Podell, and M. Lovell. Lateralization of frontal lobe functions and cognitive novelty. *Journal of Neuropsychiatry and Clinical Neurosciences*, 6:371–378, 1994. ISSN 08950172. doi:[10.1176/JNP.6.4.371](https://doi.org/10.1176/JNP.6.4.371). URL [/record/1995-12594-001](https://doi.org/10.1176/JNP.6.4.371).
- [6] Elkhonon Goldberg, Donovan Roediger, N Erkut Kucukboyaci, Chad Carlson, Orrin Devinsky, Ruben Kuzniecky, Eric Halgren, and Thomas Thesen. Hemispheric asymmetries of cortical volume in the human brain. *Cortex*, 49: 200–210, 2013. ISSN 00109452. doi:[10.1016/j.cortex.2011.11.002](https://doi.org/10.1016/j.cortex.2011.11.002). URL [http://dx.doi.org/10.1016/j.cortex.2011.11.002](https://doi.org/10.1016/j.cortex.2011.11.002).
- [7] Chandramouli Rajagopalan and Gideon Kowadlo. Bilateral brain (v1.0) [computer software], 2022. URL <https://github.com/Cerenaut/bilateral-brain>.
- [8] Anna C. Schapiro, James L. McClelland, Stephen R. Welbourne, Timothy T. Rogers, and Matthew A. Lambon Ralph. Why bilateral damage is worse than unilateral damage to the brain. *Journal of Cognitive Neuroscience*,

25:2107–2123, 12 2013. ISSN 0898-929X. doi:[10.1162/JOCN_A_00441](https://doi.org/10.1162/JOCN_A_00441). URL <https://direct.mit.edu/jocn/article/25/12/2107/28012/Why-Bilateral-Damage-Is-Worse-than-Unilateral>.

[9] Orna Peleg, Larry Manevitz, Hananel Hazan, and Zohar Eviatar. Two hemispheres—two networks: a computational model explaining hemispheric asymmetries while reading ambiguous words. *Annals of Mathematics and Artificial Intelligence* 2010 59:1, 59:125–147, 8 2010. ISSN 1573-7470. doi:[10.1007/S10472-010-9210-1](https://doi.org/10.1007/S10472-010-9210-1). URL <https://link.springer.com/article/10.1007/s10472-010-9210-1>.

[10] James A. Reggia, Sharon Goodall, and Yuri Shkuro. Computational studies of lateralization of phoneme sequence generation. *Neural Computation*, 10:1277–1297, 7 1998. ISSN 0899-7667. doi:[10.1162/089976698300017458](https://doi.org/10.1162/089976698300017458). URL <https://direct.mit.edu/neco/article/10/5/1277/6196/Computational-Studies-of-Lateralization-of-Phoneme>.

[11] Panqu Wang and Garrison Cottrell. A computational model of the development of hemispheric asymmetry of face processing. *Proceedings of the Annual Meeting of the Cognitive Science Society*, 35:35, 2013. ISSN 1069-7977.

[12] Padraic Monaghan, Richard Shillcock, and Scott McDonald. Hemispheric asymmetries in the split-fovea model of semantic processing. *Brain and Language*, 88:339–354, 3 2004. ISSN 0093-934X. doi:[10.1016/S0093-934X\(03\)00165-2](https://doi.org/10.1016/S0093-934X(03)00165-2).

[13] Padraic Monaghan and Richard Shillcock. Hemispheric dissociation and dyslexia in a computational model of reading. *Brain and Language*, 107:185–193, 12 2008. ISSN 0093-934X. doi:[10.1016/J.BANDL.2007.12.005](https://doi.org/10.1016/J.BANDL.2007.12.005).

[14] Janet Hui Wen Hsiao, Danke X. Shieh, and Garrison W. Cottrell. Convergence of the visual field split: Hemispheric modeling of face and object recognition. *Journal of Cognitive Neuroscience*, 20:2298–2307, 12 2008. ISSN 0898929X. doi:[10.1162/JOCN.2008.20162](https://doi.org/10.1162/JOCN.2008.20162).

[15] M. N. Dailey and G. W. Cottrell. Organization of face and object recognition in modular neural network models. *Neural Networks*, 12:1053–1074, 10 1999. ISSN 0893-6080. doi:[10.1016/S0893-6080\(99\)00050-7](https://doi.org/10.1016/S0893-6080(99)00050-7).

[16] Richard Shillcock and Padraic Monaghan. The computational exploration of visual word recognition in a split model. *Neural Computation*, 13:1171–1198, 5 2001. ISSN 08997667. doi:[10.1162/08997660151134370](https://doi.org/10.1162/08997660151134370).

[17] Padraic Monaghan and Richard Shillcock. Hemispheric asymmetries in cognitive modeling: connectionist modeling of unilateral visual neglect. *Psychological review*, 111:283–308, 4 2004. ISSN 0033-295X. doi:[10.1037/0033-295X.111.2.283](https://doi.org/10.1037/0033-295X.111.2.283). URL <https://pubmed.ncbi.nlm.nih.gov/15065911/>.

[18] M. A. Lambon Ralph, J. L. McClelland, K. Patterson, C. J. Galton, and J. R. Hodges. No right to speak? the relationship between object naming and semantic impairment: neuropsychological evidence and a computational model. *Journal of Cognitive Neuroscience*, 13:341–356, 4 2001. ISSN 0898-929X. doi:[10.1162/08989290151137395](https://doi.org/10.1162/08989290151137395). URL <https://direct.mit.edu/jocn/article/13/3/341/3557/No-Right-to-Speak-The-Relationship-between-Object>.

[19] Amir Mayan, Gideon Kowadlo, and Levin Kuhlmann. Right and left neural networks – inspired by the bicameral brain, 2021.

[20] Shawn Beaulieu, Lapo Frati, Thomas Miconi, Joel Lehman, Kenneth O Stanley, Jeff Clune, and Nick Cheney. Learning to continually learn. volume 325, pages 992–1001. {IOS} Press, 2020. doi:[10.3233/FAIA200193](https://doi.org/10.3233/FAIA200193). URL <https://doi.org/10.3233/FAIA200193>.

[21] Shahab Bakhtiari, Patrick Mineault, Tim Lillicrap, Christopher C Pack, and Blake A Richards. The functional specialization of visual cortex emerges from training parallel pathways with self-supervised predictive learning. *bioRxiv*, page 2021.06.18.448989, 2021. URL <https://www.biorxiv.org/content/10.1101/2021.06.18.448989v1%0Ahttps://www.biorxiv.org/content/10.1101/2021.06.18.448989v1%0Ahttps://www.biorxiv.org/content/10.1101/2021.06.18.448989v1%0Ahttps://www.biorxiv.org/content/10.1101/2021.06.18.448989v1>.

[22] Chenguang Li and Arturo Deza. What matters in branch specialization? using a toy task to make predictions. 2021. URL <https://openreview.net/forum?id=0kPS1i6wict>.

[23] Omer Sagi and Lior Rokach. Ensemble learning: A survey. *Wiley Interdisciplinary Reviews: Data Mining and Knowledge Discovery*, 8:e1249, 7 2018. ISSN 1942-4795. doi:[10.1002/WIDM.1249](https://doi.org/10.1002/WIDM.1249). URL <https://onlinelibrary.wiley.com/doi/full/10.1002/widm.1249https://onlinelibrary.wiley.com/doi/abs/10.1002/widm.1249https://wires.onlinelibrary.wiley.com/doi/10.1002/widm.1249>.

[24] Jin Tian, Minqiang Li, Fuzan Chen, and Jisong Kou. Coevolutionary learning of neural network ensemble for complex classification tasks. *Pattern Recognition*, 45:1373–1385, 4 2012. ISSN 0031-3203. doi:[10.1016/J.PATCOG.2011.09.012](https://doi.org/10.1016/J.PATCOG.2011.09.012).

[25] Stefan Lee, Senthil Purushwalkam, Michael Cogswell, David Crandall, and Dhruv Batra. Why m heads are better than one: Training a diverse ensemble of deep networks. 11 2015. doi:[10.48550/arxiv.1511.06314](https://arxiv.org/abs/1511.06314). URL <https://arxiv.org/abs/1511.06314v1>.

[26] Kazi Md Rokibul Alam, Nazmul Siddique, and Hojjat Adeli. A dynamic ensemble learning algorithm for neural networks. *Neural Computing and Applications*, 32:8675–8690, 6 2020. ISSN 14333058. doi:[10.1007/s00521-019-04359-7](https://doi.org/10.1007/s00521-019-04359-7). URL <https://link.springer.com/article/10.1007/s00521-019-04359-7>.

[27] Rui He, Shengcui Liu, Shan He, and Ke Tang. Multi-Domain Active Learning: Literature Review and Comparative Study, October 2022. URL [http://arxiv.org/abs/2106.13516](https://arxiv.org/abs/2106.13516). arXiv:2106.13516 [cs].

[28] Mahesh Joshi, Mark Dredze, William Cohen, and Carolyn Rose. Multi-domain learning: when do domains matter? In *Proceedings of the 2012 Joint Conference on Empirical Methods in Natural Language Processing and Computational Natural Language Learning*, pages 1302–1312, 2012.

[29] Yimin Chen, Rongrong Lu, Yibo Zou, and Yanhui Zhang. Branch-activated multi-domain convolutional neural network for visual tracking. *Journal of Shanghai Jiaotong University (Science)*, 23:360–367, 2018.

[30] Alex Krizhevsky. Learning multiple layers of features from tiny images, 2009.

[31] Jia Deng, Wei Dong, Richard Socher, Li-Jia Li, Kai Li, and Li Fei-Fei. Imagenet: A large-scale hierarchical image database. pages 248–255, 3 2010. doi:[10.1109/CVPR.2009.5206848](https://doi.org/10.1109/CVPR.2009.5206848).

[32] Brenden M Lake, Ruslan Salakhutdinov, and Joshua B Tenenbaum. Human-level concept learning through probabilistic program induction. *Science*, 350:1332–1338, 2015. ISSN 10959203. doi:[10.1126/science.aab3050](https://doi.org/10.1126/science.aab3050).

[33] Eleni Triantafillou, Tyler Zhu, Vincent Dumoulin, Pascal Lamblin, Utku Evci, Kelvin Xu, Ross Goroshin, Carles Gelada, Kevin Swersky, Pierre-Antoine Manzagol, and Hugo Larochelle. Meta-dataset: A dataset of datasets for learning to learn from few examples. 3 2020. doi:[10.48550/arxiv.1903.03096](https://arxiv.org/abs/1903.03096). URL <https://arxiv.org/abs/1903.03096v4>.

[34] Massimo Caccia, Pau Rodriguez, Oleksiy Ostapenko, Fabrice Normandin, Min Lin, Lucas Page-Caccia, Isam Hadj Laradji, Irina Rish, Alexandre Lacoste, David Vázquez, and Laurent Charlin. Online fast adaptation and knowledge accumulation (osaka): a new approach to continual learning. *Advances in Neural Information Processing Systems*, 33:16532–16545, 2020. URL <https://github.com/ElementAI/osaka>.

[35] Kaiming He, Xiangyu Zhang, Shaoqing Ren, and Jian Sun. Deep residual learning for image recognition. *Proceedings of the IEEE Computer Society Conference on Computer Vision and Pattern Recognition*, 2016-Decem:770–778, 9 2015. ISSN 10636919. doi:[10.48550/arxiv.1512.03385](https://arxiv.org/abs/1512.03385). URL <https://arxiv.org/abs/1512.03385v1>.

[36] Karen Simonyan and Andrew Zisserman. Very Deep Convolutional Networks for Large-Scale Image Recognition, April 2015. URL [http://arxiv.org/abs/1409.1556](https://arxiv.org/abs/1409.1556). arXiv:1409.1556 [cs].

[37] Arild Nøkland and Lars Hiller Eidnes. Training Neural Networks with Local Error Signals, May 2019. URL [http://arxiv.org/abs/1901.06656](https://arxiv.org/abs/1901.06656). arXiv:1901.06656 [cs, stat].

[38] Nitish Srivastava, Geoffrey Hinton, Alex Krizhevsky, Ilya Sutskever, and Ruslan Salakhutdinov. Dropout: A simple way to prevent neural networks from overfitting. *Journal of Machine Learning Research*, 15:1929–1958, 2014.

[39] Diederik P Kingma and Jimmy Ba. Adam: A method for stochastic optimization. 9 2014. URL [http://arxiv.org/abs/1412.6980](https://arxiv.org/abs/1412.6980).

[40] William Falcon and contributors. Pytorch lightning (v1.4.1) [computer software], 2019. URL <https://github.com/PyTorchLightning/pytorch-lightning>.

[41] Adam Paszke, Sam Gross, Francisco Massa, Adam Lerer, James Bradbury, Gregory Chanan, Trevor Killeen, Zeming Lin, Natalia Gimelshein, Luca Antiga, Alban Desmaison, Andreas Köpf, Edward Yang, Zach DeVito, Martin Raison, Alykhan Tejani, Sasank Chilamkurthy, Benoit Steiner, Lu Fang, Junjie Bai, and Soumith Chintala. Pytorch: An imperative style, high-performance deep learning library. *Advances in Neural Information Processing Systems*, 32, 2019. ISSN 10495258.

[42] Aditya Chattopadhyay, Anirban Sarkar, Prantik Howlader, and Vineeth N Balasubramanian. Grad-cam++: Improved visual explanations for deep convolutional networks. 9 2017. doi:[10.1109/WACV.2018.00097](https://doi.org/10.1109/WACV.2018.00097). URL [http://arxiv.org/abs/1710.11063](https://arxiv.org/abs/1710.11063)[http://dx.doi.org/10.1109/WACV.2018.00097](https://doi.org/10.1109/WACV.2018.00097).

[43] Ramprasaath R Selvaraju, Michael Cogswell, Abhishek Das, Ramakrishna Vedantam, Devi Parikh, and Dhruv Batra. Grad-cam: Visual explanations from deep networks via gradient-based localization. 9 2016. doi:[10.1007/s11263-019-01228-7](https://doi.org/10.1007/s11263-019-01228-7). URL [http://arxiv.org/abs/1610.02391](https://arxiv.org/abs/1610.02391)[http://dx.doi.org/10.1007/s11263-019-01228-7](https://doi.org/10.1007/s11263-019-01228-7).

[44] Jacob Gildenblat and contributors. Pytorch library for cam methods (v1.4.5) [computer software], 2021. URL <https://github.com/jacobgil/pytorch-grad-cam>.

[45] Richard G. Carson. Inter-hemispheric inhibition sculpts the output of neural circuits by co-opting the two cerebral hemispheres. *The Journal of Physiology*, 598:4781–4802, 11 2020. ISSN 1469-7793. doi:10.1113/JP279793. URL <https://onlinelibrary.wiley.com/doi/full/10.1113/JP279793><https://onlinelibrary.wiley.com/doi/abs/10.1113/JP279793><https://physoc.onlinelibrary.wiley.com/doi/10.1113/JP279793>.

[46] Gorana Pobric, Nira Mashal, Miriam Faust, and Michal Lavidor. The role of the right cerebral hemisphere in processing novel metaphoric expressions: A transcranial magnetic stimulation study. *Journal of Cognitive Neuroscience*, 20:170–181, 1 2008. ISSN 0898-929X. doi:10.1162/JOCN.2008.20005. URL <https://direct.mit.edu/jocn/article/20/1/170/4440/The-Role-of-the-Right-Cerebral-Hemisphere-in>.

[47] James L McClelland, Bruce L McNaughton, and Randall C O'Reilly. Why there are complementary learning systems in the hippocampus and neocortex: Insights from the successes and failures of connectionist models of learning and memory. *Psychological Review*, 102:419–457, 1995. ISSN 0033295X. doi:10.1037/0033-295X.102.3.419.

[48] Randall C O'Reilly, Rajan Bhattacharyya, Michael D Howard, and Nicholas Ketz. Complementary learning systems. *Cognitive Science*, 38:1229–1248, 2014. ISSN 03640213. doi:10.1111/j.1551-6709.2011.01214.x.

[49] Olivia A. Shipton, Mohamady El-Gaby, John Apergis-Schoute, Karl Deisseroth, David M. Bannerman, Ole Paulsen, and Michael M. Kohl. Left-right dissociation of hippocampal memory processes in mice. *Proceedings of the National Academy of Sciences of the United States of America*, 111:15238–15243, 10 2014. ISSN 10916490. doi:10.1073/PNAS.1405648111/SUPPL_FILE/PNAS.201405648SI.PDF. URL <https://www.pnas.org/doi/abs/10.1073/pnas.1405648111>.

[50] Mohamady El-Gaby, Olivia A. Shipton, and Ole Paulsen. Synaptic plasticity and memory. <http://dx.doi.org/10.1177/1073858414550658>, 21:490–502, 9 2014. ISSN 10894098. doi:10.1177/1073858414550658. URL <https://journals.sagepub.com/doi/abs/10.1177/1073858414550658>.

[51] Robert L. Sainburg. Handedness: Differential specializations for control of trajectory and position. *Exercise and Sport Sciences Reviews*, 33:206–213, 10 2005. ISSN 0091-6331. doi:10.1097/00003677-200510000-00010. URL <https://pennstate.pure.elsevier.com/en/publications/handedness-differential-specializations-for-control-of-trajectory>.

[52] Elkhonon. Goldberg. *The new executive brain: frontal lobes in a complex world*. Oxford University Press, 2009. ISBN 9780195329407.